Invariant Thr^{244} is essential for the efficient acylation step of the non-phosphorylating glyceraldehyde-3-phosphate dehydrogenase from *Streptococcus mutans*

Arnaud PAILOT*, Katia D'AMBROSIO†‡, Catherine CORBIER†, François TALFOURNIER*[1] and Guy BRANLANT*[1]

*MAEM, UMR 7567 Nancy-Université, CNRS, Faculté des Sciences, 54506 Vandoeuvre Cedex, France, †LCM3B, Groupe Biocristallographie, UMR 7036 Nancy-Université, CNRS, Faculté des Sciences, 54506 Vandoeuvre Cedex, France, and ‡Istituto di Biostrutture e Bioimmagini, CNR, 80134 Napoli, Italy

One of the most striking features of several X-ray structures of CoA-independent ALDHs (aldehyde dehydrogenases) in complex with NAD(P) is the conformational flexibility of the NMN moiety. However, the fact that the rate of the acylation step is high in GAPN (non-phosphorylating glyceraldehyde-3-phosphate dehydrogenase) from *Streptococcus mutans* implies an optimal positioning of the nicotinamide ring relative to the hemithioacetal intermediate within the ternary GAPN complex to allow an efficient and stereospecific hydride transfer. Substitutions of serine for invariant Thr^{244} and alanine for Lys^{178} result in a drastic decrease of the efficiency of hydride transfer which becomes rate-limiting. The crystal structure of the binary complex T244S GAPN–NADP shows that the absence of the β-methyl group leads to a well-defined conformation of the NMN part, including the nicotinamide ring, clearly different from that depicted to be suitable for an efficient hydride transfer in the wild-type. The $\sim$0.6-unit increase in pK_{app} of the catalytic Cys^{302} observed in the ternary complex for both mutated GAPNs is likely to be due to a slight difference in positioning of the nicotinamide ring relative to Cys^{302} with respect to the wild-type ternary complex. Taken together, the data support a critical role of the Thr^{244} β-methyl group, held in position through a hydrogen-bond interaction between the Thr^{244} β-hydroxy group and the ε-amino group of Lys^{178}, in permitting the nicotinamide ring to adopt a conformation suitable for an efficient hydride transfer during the acylation step for all the members of the CoA-independent ALDH family.

Key words: acylation step, aldehyde dehydrogenase (ALDH), hydride transfer, nicotinamide conformation, *Streptococcus mutans*, X-ray structure.

INTRODUCTION

Non-phosphorylating ALDHs (aldehyde dehydrogenases) belong to a family of phylogenetically and structurally related enzymes that catalyse the NAD(P)-dependent oxidation of a wide variety of aldehydes to their corresponding non-activated or CoA-activated acids. ALDHs are known to participate in many biological functions, such as intermediary metabolism, detoxification, osmotic protection and cellular differentiation. They share a similar chemical mechanism involving two major steps: first, an acylation step common to both families and, second, a deacylation step that differs by the nature of the acyl acceptor. The acylation step involves the formation of a thiohemiacetal intermediate via nucleophilic attack of the catalytic Cys^{302} on the aldehydic function followed by an oxidoreduction process leading to the formation of a thioacylenzyme intermediate and NAD(P)H. (The amino acid numbering used for the biochemical and structural data is that defined by Wang and Weiner [1], and this nomenclature has been used for all biochemical studies performed on members of the ALDH family.) The deacylation step includes the nucleophilic attack of a water or CoA molecule on the thioacylenzyme intermediate and release of the non-activated or CoA-activated acids. Moreover, previous studies have highlighted major differences in the kinetic mechanism of ALDHs depending upon the nature of the deacylation step. In CoA-independent ALDHs, kinetic data support an ordered sequential mechanism in which NAD(P)H dissociates last [2,3], whereas CoA-dependent ALDHs exhibit a Ping Pong mechanism in which the release of the reduced cofactor occurs before the *trans*-thioesterification step [4,5].

Mechanistic aspects were studied extensively for CoA-independent ALDHs, and several invariant residues were shown to be critical for the chemical mechanism [1,6–8]. In addition, evidence has been provided for the chemical activation of catalytic Cys^{302} upon cofactor binding to GAPN (non-phosphorylating glyceraldehyde-3-phosphate dehydrogenase) from *Streptococcus mutans* through a local conformational rearrangement which has been shown to be strongly kinetically favoured by substrate binding to the binary complex GAPN–NADP [9]. Moreover, enzymatic and structural studies on GAPN and other ALDHs have highlighted the essential roles of: (i) an oxyanion hole composed of the side chain of invariant Asn^{169} and the main-chain nitrogen of Cys^{302} that allows an efficient hydride transfer without base catalyst assistance [10–13], and (ii) invariant Glu^{268} in the rate-limiting hydrolysis step through activation and orientation of the attacking water molecule [2]. Additionally, numerous crystal structures of CoA-independent ALDHs have already been solved in the presence of NAD(P). One of the most striking features of many ALDH structures is the conformational flexibility of the NMN moiety of the cofactor, which is seen as having missing or weak electron density (see, e.g., [11,14–15]). However, two discrete conformations, compatible with the two-step catalytic mechanism, were described for class 1 and class 2 ALDHs [10,16]. In the

Abbreviations used: ALDH, aldehyde dehydrogenase; GAPN, non-phosphorylating glyceraldehyde-3-phosphate dehydrogenase; G3P, glyceraldehyde 3-phosphate; 2PDS, 2,2′-dipyridyl disulfide; r.m.s.d., root mean square deviation.

[1] Correspondence may be addressed to either of these authors (email francois.talfournier@maem.uhp-nancy.fr or guy.branlant@maem.uhp-nancy.fr).

Co-ordinates and structural factors for T244S mutant GAPN (non-phosphorylating glyceraldehyde-3-phosphate dehydrogenase) have been deposited in the Protein Data Bank under accession code 2ID2.

first conformation, the NMN moiety, in particular that of the nicotinamide ring, occupies a position suitable for hydride transfer, but not for deacylation because it would sterically exclude catalytic Glu^{268} from playing its role in the hydrolytic process. The fact that the cofactor remains bound to the enzyme along the two-step catalytic mechanism, strongly suggested that movement of the reduced NMN (NMNH) is a prerequisite for completion of the second half of the reaction. The second conformation in which the NMN moiety adopts a contracted position was hypothesized to be suitable for hydrolysis. This view was supported by comparison of human ALDH2 structures in complex with either NAD or NADH, which provided arguments in favour of a conformational preference for the oxidized and reduced cofactors [17]. Recently, the first structural evidence for a conformational isomerization of the cofactor during the catalytic cycle of CoA-independent ALDH was put forward by the crystal structure of a GAPN thioacylenzyme intermediate–NADPH complex [18]. This structure revealed that the reduced cofactor adopts a new conformation with a flip of the NMNH moiety which has been proposed to be suitable for the deacylation step for all members of the CoA-independent ALDH family. In contrast, the key question about the positioning of the nicotinamide ring during the acylation step and the structural factors involved remains to be addressed. In the case of GAPN from *S. mutans*, inspection of the three-dimensional structure of the binary complex GAPN–NADP revealed a poorly defined electron density around the NMN portion. The fact that the rate of the acylation step is high ($> 500\ s^{-1}$) is, however, indicative of a defined positioning of the nicotinamide ring relative to the transient hemithioacetal intermediate competent for an efficient hydride transfer [2]. In the conformation depicted to be suitable for an efficient hydride transfer in CoA-independent ALDHs, including GAPN, the nicotinamide ring is positioned between Cys^{302} and the β-methyl group of the invariant Thr^{244} residue, each at a distance of ~ 3.5 Å (1 Å = 0.1 nm) from the ring [10,11,17]. This suggested a major role of the β-methyl group of Thr^{244} in the positioning of the nicotinamide ring within the covalent ternary complex. Such an assumption is also supported by the fact that the Thr^{244} side chain could be held in position through hydrogen-bond interaction between its β-hydroxy group and the ε-amino group of Lys^{178}, a residue highly conserved in all known primary structures of CoA-independent ALDHs.

In the present study, the catalytic properties of the T244S, T244V and K178A mutated GAPNs were determined. These substitutions result in a drastic effect on the acylation step, which becomes rate-limiting for the overall reaction in contrast with the wild-type for which the deacylation step is rate-limiting. Moreover, the crystal structure of a binary complex T244S GAPN–NADP shows that the NMN moiety of the NADP molecule is now well defined in the electron-density maps. The nicotinamide ring adopts a unique conformation clearly different from that hypothesized to be operative in the ALDH–GAPN acylating ternary complex [10,15–17]. Taken together, these results support a critical role of Thr^{244}, in particular of its β-methyl group, in permitting the nicotinamide ring to adopt a conformation suitable for efficient hydride transfer. All the results are discussed in relation to available data on the CoA-independent ALDH family and for their relevance to the two-step catalytic mechanism.

EXPERIMENTAL

Production and purification of mutated GAPNs from *S. mutans*, and materials

T244S, T244S/C382S, T244V and K178A mutated GAPNs were produced as described previously [9]. For purification, cells were harvested by centrifugation at 3000 ***g*** for 20 min, resuspended in 50 mM potassium phosphate buffer, pH 8.2 (buffer A) and disrupted by sonication for 5 min using a Branson Sonifier 250. The extract was clarified by centrifugation at 15000 ***g*** for 90 min, and solid ammonium sulfate was added to either 40 % saturation for T244S and T244S/C382S GAPNs or 30 % saturation for T244V and K178A. The precipitate was removed by centrifugation at 15000 ***g*** for 90 min, and the supernatant was applied to a high-performance phenyl-Sepharose column using a FPLC system (Amersham Biosciences) equilibrated previously with buffer A containing 1 M ammonium sulfate. Following equilibration, mutated GAPNs were eluted using a descending gradient (1–0 M) of ammonium sulfate at $5\ ml \cdot min^{-1}$. Fractions containing mutated GAPNs were pooled, concentrated and dialysed exhaustively against buffer A and applied to a Q-Sepharose column equilibrated with buffer A. After washing with buffer A, mutated GAPNs were eluted using a 0–1 M KCl gradient at $5\ ml \cdot min^{-1}$. At this stage, mutated GAPNs were considered to be pure as judged by SDS/7.5 % PAGE and by electrospray-MS analysis. T244V and K178A GAPNs were isolated as apo forms, whereas 0.8 mol of NADP remained bound per tetramer of T244S and T244S/C382S GAPNs. Enzyme concentrations were determined spectrophotometrically as the apo form by using a molar absorption coefficient of $2.04 \times 10^5\ M^{-1} \cdot cm^{-1}$ at 280 nm [9] and are expressed in molarity. All other materials were reagent-grade or better and were used without further purification. NADP (Roche) was dissolved in water, and the stock concentration was determined spectrophotometrically by using a molar absorption coefficient of $18000\ M^{-1} \cdot cm^{-1}$ at 259 nm. D,L-G3P (G3P is glyceraldehyde 3-phosphate) or D-G3P (Sigma) was obtained by hydrolysing D,L-G3P diethyl acetal or D-G3P diethyl acetal respectively, according to the manufacturer's instructions, and its concentration was assessed enzymatically using wild-type GAPN.

Quantification of NADP content

The NADP content of purified GAPNs was quantified enzymatically after addition of 0.2 mM D,L-G3P to 1.25 μM GAPN by following the appearance of NADPH on a SAFAS flx spectrofluorometer. Fluorescence measurements were carried out in 50 mM potassium phosphate buffer at pH 8.2. The excitation wavelength was set at 358 nm, and spectra were recorded in the range 380–540 nm. Maximum emission intensity was observed at 460 nm.

Steady-state kinetic analyses

Initial rate measurements were carried out on a Kontron Uvikon 933 spectrophotometer by following the appearance of NADPH at 340 nm. Determination of the kinetic parameters was carried out at the optimum pH of 8.2 in 50 mM Tes buffer and 5 mM 2-mercaptoethanol. The temperature of the solutions was maintained at 25 °C by thermostatically controlled sample holders using a circulating water bath for all measurements. Catalytic constants k_{cat} and K_m were determined by measuring steady-state velocity at various D,L-G3P and NADP concentrations under conditions where no inhibitory effect was observed either with NADP or D,L-G3P. Data were plotted according to the Michaelis–Menten equation using least-squares regression analysis.

Deuterium isotope effects

D-[1-^{2}H]G3P was prepared as described previously [19] and its concentration was determined enzymatically. Isotopic effects on T244S and K178A GAPNs were measured in 50 mM Tes buffer, pH 8.2, and 5 mM 2-mercaptoethanol by direct comparison of the initial velocities measured with D-G3P and D-[1-^{2}H]G3P at

concentrations of 0.1 and 0.2 mM for both mutated GAPNs in the presence of NADP at 25 °C.

pH-dependence of the steady-state rate constant of K178A and T244S GAPNs

The pH-dependence of the steady-state rate constant, k_{cat}, which was shown to be associated with the rate-limiting acylation step (see the Results section), was studied over the pH range 5.25–8.75 or 5.25–9.00 in a mixed reaction buffer consisting of 120 mM Tris, 30 mM imidazole and 30 mM ethanoic (acetic) acid (pH-adjusted with NaOH or HCl), adjusted with 3 M NaCl to a constant ionic strength of 0.15 M. The apparent pK_a parameters governing the pH-dependence of k_{cat} were extracted from k_{obs} against pH profiles and analysed as described by Marchal and Branlant [9].

Kinetic reactions with 2PDS (2,2′-dipyridyl disulfide)

Owing to the high reactivity of cysteine residues in all mutated GAPNs, kinetic measurements were carried out on a SX18MV-R Applied Photophysics stopped-flow apparatus (Leatherhead) at 25 °C, under pseudo-first-order conditions in 30 mM ethanoic acid, 30 mM imidazole and 120 mM Tris buffer at a constant ionic strength of 0.15 M over the pH range 5.50–8.75 for T244S and T244/C382S GAPNs and 5.75–9.25 for K178A GAPN. The pH range was used to study the pH stability of the mutated GAPNs. One syringe contained the apo or apo-like form of GAPN, and the other contained 2PDS. (In contrast with the term 'holo form', the term 'apo-like form' indicates here an apo form saturated by NADP but in which the cofactor has not yet induced the local conformational rearrangement of the active site, including the decrease of the pK_a of Cys^{302} and the loss of the salt-bridge between Glu^{268} and Arg^{459} [9,15].) The reaction was monitored at 343 nm with 2.5 μM GAPN and 200 μM 2PDS and pyridine-2-thione was quantified using an molar absorption coefficient of 8080 $M^{-1} \cdot cm^{-1}$. The pseudo-first-order k_{obs} values were determined at each pH by fitting the absorbance A at 343 nm against time t to a monophasic expression (eqn 1):

$$A_{343} = a(1 - e^{-k_{obs} \times t}) + c \quad (1)$$

where k_{obs} is the observed rate constant, a is the burst magnitude and c represents the value of the ordinate intercept, or to a biphasic expression (eqn 2):

$$A_{343} = a_1(1 - e^{-k_{obs1} \times t}) + a_2(1 - e^{-k_{obs2} \times t}) + c \quad (2)$$

where k_{obs1} and k_{obs2} are the observed rate constants for the fast and the slower phase respectively, a_1 and a_2 are the relative amplitude values for the two phases, and c represents the value of the ordinate intercept.

The second-order rate constants, k_2, were determined at each pH value and data were analysed as described by Marchal and Branlant [9].

Crystallization, data collection and processing

Crystals of the T244S GAPN with NADP were obtained using the hanging-drop vapour-diffusion method at 293 K. A 2–6 μl volume of a 5 $mg \cdot ml^{-1}$ protein solution in 50 mM imidazole buffer at pH 6.8 was mixed with 1–2 μl of reservoir solution composed of 1.9–2.0 M ammonium sulfate, 0.1 M Hepes buffer, pH 7.5, and 2 % PEG [poly(ethylene glycol)] 400 [12,15]. The crystals grew within a few days. A 2.50 Å resolution data set was collected at 100 K at the synchrotron source in Trieste. The crystals belong to the space group $P2_12_12$, with unit cell dimensions $a = 143.7$ Å, $b = 154.4$ Å and $c = 115.0$ Å. Diffracted data were processed using the HKL crystallographic data reduction package [20]. Statistics of the data set are summarized in Table 1.

Table 1 Data collection and refinement statistics

Values in parentheses refer to the outermost resolution shell.

(a) Data collection

Parameter	Value
Space group	$P2_12_12$
a (Å)	143.7
b (Å)	154.4
c (Å)	115.0
Z	4
Resolution (Å)	2.5 (2.59–2.50)
Temperature (K)	100
Total reflections	323 307
Independent reflections	78 424
Completeness (%)	88.2 (90.1)
R-sym	10.4 (37)
$I/\sigma(I)$	11.7 (4.5)

(b) Refinement

Parameter	Value
R-factor (%)	17.6
R-free (%)	22.7
R.m.s.d. from ideal geometry:	
Bond lengths (Å)	0.005
Bond angles (°)	1.26
Average B-factor (Å^2)	
Main chain	24.3
Side chains	27.9
Water molecules	26.4
NADP (AMP moiety)	28.98
NADP (NMN)	32.87

Phasing, refinement and quality of the model

The structure of T244S GAPN was solved by difference Fourier techniques, using the wild-type apo-like structure as a starting model (PDB code 2EUH) [15].

Several cycles of rigid-body refinement carried out with CNS [21] led to a decrease in the crystallographic R-factor and R-free values to 0.23 and 0.28 respectively. The analysis of the $(2F_o - F_c)$ electron-density map at this stage of refinement was very well defined for all the structure, including the mutated residue. The ordered water molecules were added automatically and checked individually. Moreover, seven sulfate ions were added (one in each of the A and C monomers, two in the B monomer and three in the D monomer) and refined with occupancy factors ranging from 0.5 to 1. After refinement (CNS) and manual rebuilding (Turbo-Frodo; Silicon Graphics) the final crystallographic R-factor and R-free values calculated for the 78 424 independent reflections (in the 20.00–2.50 Å resolution range) were 0.176 and 0.227 respectively. The stereochemical quality of the model was assessed using PROCHECK [23]. The most favoured and additionally allowed regions of the Ramachandran plot contained 99.6 % of the non-glycine residues. The final model consisted of 14 362 non-hydrogen atoms, 1109 water molecules and seven sulfate ions coming from the crystallization solution. The refined structure presented a good geometry with r.m.s.d. (root mean square deviation) from ideal bond lengths and angles of 0.005 Å and 1.26° respectively. The average temperature factor (B) for all atoms was 24.6 Å^2.

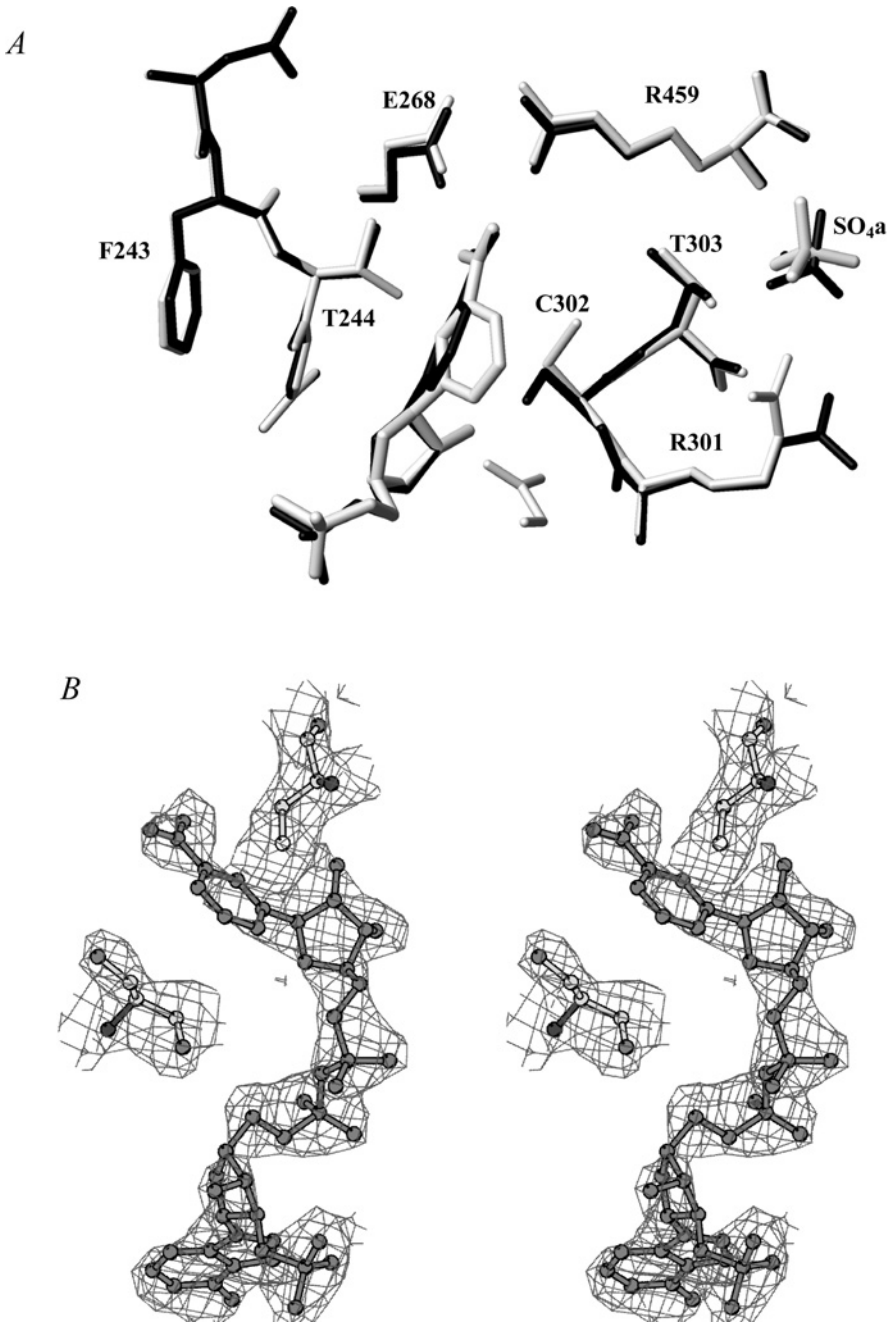

Figure 1 Active site of T244S GAPN

(**A**) Superimposition of the active-site regions of the apo-like wild-type enzyme (in grey) and of the T244S GAPN (in black). The conformation of the NMN moiety in the wild-type structure is the one described to be suitable for efficient hydride transfer [9,17]. Single letter amino acid codes are used. (**B**) Stereo view of the cofactor molecule in the ($2F_o - F_c$) electron-density map (contour level: 1 σ).

The statistics for refinement and model geometry are summarized in Table 1. Figure 1(A) was drawn using MOLMOL [24] and Figure 1(B) with BOBSCRIPT [25]

RESULTS

Rationale for the mutations

As indicated in the Introduction, we have postulated that Thr^{244} and its potential interaction with Lys^{178} could be critical in the correct positioning of the NMN moiety of the cofactor during acylation, so that hydride transfer can occur with an optimum efficiency. In order to validate this assumption, the roles of Thr^{244} and Lys^{178} have been probed by site-directed mutagenesis. Introduction of a residue such as serine at position 244 would provide experimental support for the role of the van der Waals interaction between the β-methyl group of Thr^{244} and the nicotinamide ring, whereas T244V and K178A substitutions would assess the role of the Lys^{178}/Thr^{244} hydrogen-bond interaction in the correct positioning of the β-methyl group of Thr^{244} relative to the nicotinamide ring of the cofactor. In the apo and apo-like forms of GAPN, Cys^{302} and Cys^{382} were shown previously to be reactive towards 2PDS

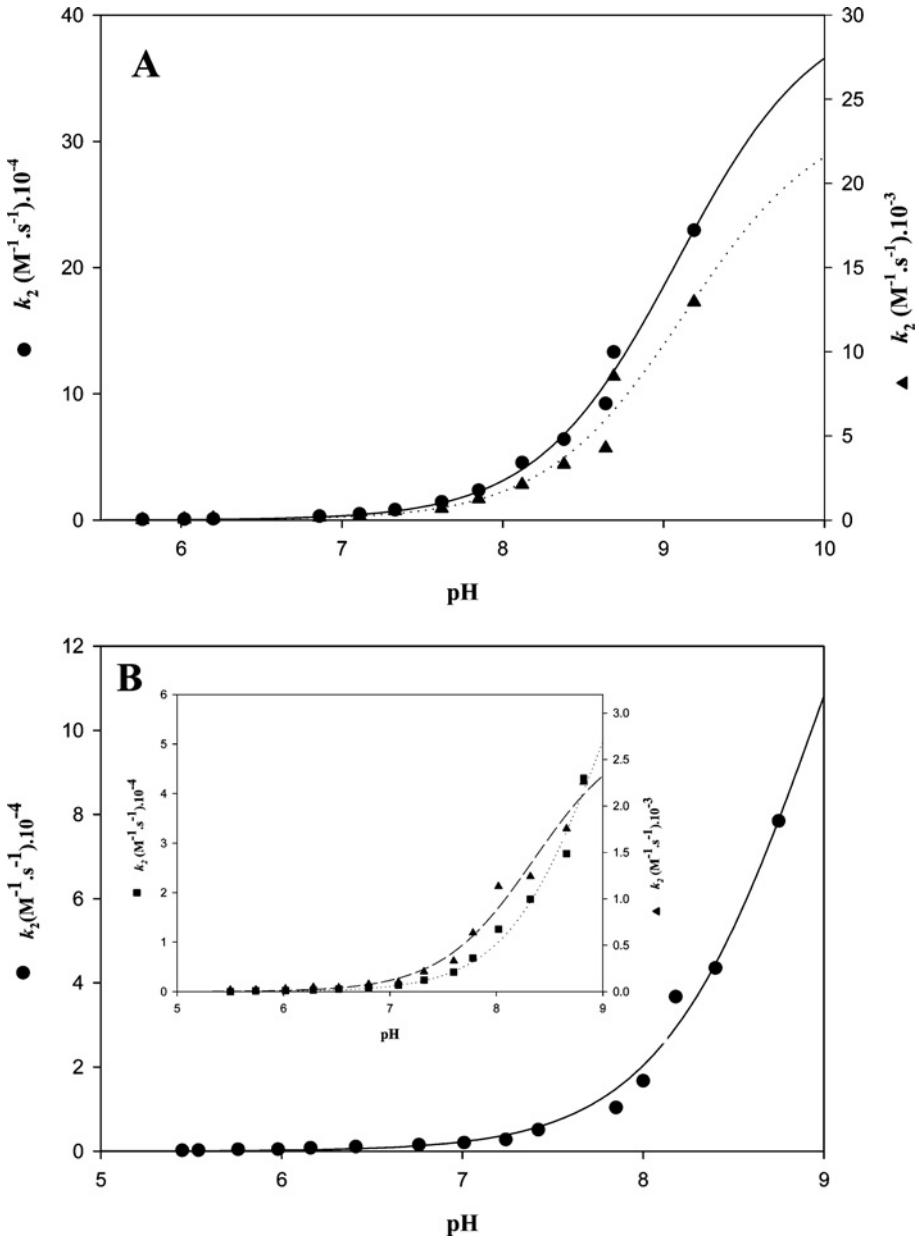

Figure 2 pH-dependence of the second-order rate constant, k_2, for the reaction of 2PDS with apo K178A and apo-like T244S and T244S/C382S GAPNs

Kinetics were determined at 25 °C as indicated in the Experimental section. The GAPN and 2PDS concentrations were 2.5 μM and 200 μM respectively. Rate constants, k_{obs}, were determined using non-linear regression analysis, and second-order rate constants, k_2, were calculated by dividing the k_{obs} values by the concentration of 2PDS. Transients obtained on the apo K178A and apo-like T244S GAPNs were analysed according to eqn (2), reflecting the contribution of Cys^{302} and Cys^{382}. Transients obtained on the apo-like T244S/C382S GAPN were analysed according to eqn (1). (**A**) Apo K178A GAPN: both data sets were fitted against a single pK_a model, which provided pK_{app} values of 8.80 and 9.15, and k_2 values of 3.3×10^5 M$^{-1} \cdot$ s^{-1} (●) and 3.05×10^4 M$^{-1} \cdot$ s^{-1} (▲) respectively. (**B**) Main panel: data sets obtained on the apo-like T244S/C382S GAPN were fitted against a single pK_a model, which provided pK_{app} and k_2 values of 9.0 and 2×10^5 M$^{-1} \cdot$ s^{-1} respectively. Inset: data sets obtained on the apo-like T244S GAPN were fitted against a single pK_a model, which provided pK_{app} values of 8.50 and 9.00 and k_2 values of 3.3×10^3 M$^{-1} \cdot$ s^{-1} (▲) and 9.5×10^4 M$^{-1} \cdot$ s^{-1} (■) respectively. S.E.M. on each experimental point was less than 5 %.

[9]. Therefore, to assign pK_{app} and k_2 values to Cys^{302} in the apo-like form of T244S GAPN, Cys^{382} has been replaced by a serine residue.

Determination of the pK_{app} values and reactivities of the cysteine residues in the apo form of K178A GAPN and apo-like forms of K178A, T244S and T244S/C382S GAPNs with 2PDS

For all mutated GAPNs, the reaction with 2PDS under native conditions obeyed pseudo-first-order kinetics with formation of 2 mol of pyridine-2-thione per subunit as determined from the A_{343} value, except that only 1 mol of 2PDS reacted per subunit of T244S/C382S GAPN. This is in agreement with what was described for the wild-type in which two residues, i.e. Cys^{302} and Cys^{382} were shown to be reactive per monomer [9]. For the K178A GAPN apo form, the two cysteine residues exhibited distinct k_2 constants. The pH–k_2 profile for each thiolate showed sigmoidal behaviour with pK_{app} values of 8.80 and 9.15 and k_2 values of 3.3×10^5 M$^{-1} \cdot$ s^{-1} and 3.05×10^4 M$^{-1} \cdot$ s^{-1} respectively (Figure 2A and Table 2). The high k_2 values indicated that both cysteine residues are

Table 2 Parameters for the pH-dependence of the second-order rate constants for the reaction of 2PDS with K178A, T244S and T244S/C382S GAPNs

The experimental conditions are described in the Experimental section. Transients obtained on the apo and apo-like K178A and apo-like T244S GAPN were best described by a double-exponential expression reflecting the contribution of Cys^{302} and Cys^{382} and data were analysed according to eqn (2). For the apo-like T244S/C382S GAPN, experimental data were best described by a mono-exponential expression according to eqn (1). The second-order rate constants at each pH were fitted to a monosigmoidal equation to determine the pK_{app} values in Sigmaplot (SPSS). The error estimates are those provided by the program. ND, not determined.

GAPN	k_2 ($M^{-1} \cdot s^{-1}$)	pK_{app}
Apo-GAPNs		
Wild-type*	1350 ± 28	8.84 ± 0.04
C382A*	225 ± 9	8.49 ± 0.07
C302A*	588 ± 14	9.07 ± 0.02
K178A	$(3.30 \pm 0.25) \times 10^5$	8.80 ± 0.07
	$(3.05 \pm 0.25) \times 10^4$	9.15 ± 0.15
Holo-GAPN		
Wild-type*	$>2 \times 10^5$	ND
Wild-type†	182 ± 2	6.1 ± 0.2
Apo-like-GAPNs‡		
K178A§	$(3.0 \pm 0.1) \times 10^5$	8.85 ± 0.05
	$(2.9 \pm 0.2) \times 10^4$	9.25 ± 0.05
T244S§	$(3.0 \pm 0.3) \times 10^3$	8.5 ± 0.1
	$(9.5 \pm 2) \times 10^4$	9.0 ± 0.2
T244S/C382S§	$(2.0 \pm 0.4) \times 10^5$	9.0 ± 0.1

* From [9].

† This pK_{app} value of 6.1 for Cys^{302} was determined using iodoacetamide as a kinetic probe (from [9]).

‡ Apo-like forms refer to GAPN/NADP binary complexes after incubation at 4 °C of the apo forms (or partially apo forms in the case of T244S and T244S/C382S GAPNs) in the presence of saturating concentration of NADP for 5 h at pH 5.5 under conditions where the conformational rearrangement occurred in the wild-type enzyme (from [9]) but not in the mutated GAPNs.

§ Although no additional experimental data can be obtained beyond the inflection point of the curves, non-linear regression analysis provides accurate pK_a values.

accessible within the active site of K178A GAPN, in contrast with what was observed for the wild-type apo form [9]. The high accessibility of Cys^{302} is probably not catalytically relevant, but rather is another example of the great conformational flexibility exhibited by this residue within the active site [9,26]. The apo form of K178A GAPN incubated at 4 °C in the presence of saturating concentrations of NADP for 5 h at pH 5.5 under conditions where the conformational rearrangement of the active site was shown to occur in the apo wild-type, displayed a similar pH–k_2 profile to that described for the apo K178A GAPN with pK_{app} values of 8.85 and 9.25 and k_2 values of 3.0×10^5 and 2.9×10^4 $M^{-1} \cdot s^{-1}$ respectively (curves not shown, see Table 2). Since the apo form of T244S GAPN could not be obtained irrespective of the experimental procedure used (results not shown), titration by 2PDS was only performed on the apo-like form of T244S GAPN after incubation for 5 h at 4 °C and pH 5.5 in the presence of saturating concentrations of NADP. A pH–k_2 profile similar to that of apo and apo-like forms of K178A GAPN was obtained with pK_{app} values of 8.5 and 9.0 and k_2 values of 3×10^3 and 9.5×10^4 $M^{-1} \cdot s^{-1}$ respectively (Figure 2B, inset, and Table 2). The pH–k_2 curve of the apo-like form of T244S/C382S GAPN fitted only to a monosigmoidal profile with a pK_{app} value of 9.0 and a k_2 value of 2×10^5 $M^{-1} \cdot s^{-1}$ (Figure 2B and Table 2). Such a result strongly suggests that the pK_{app} of 9.0 determined in the T244S GAPN represents that of Cys^{302}.

Kinetic properties of T244S, T244V and K178A GAPNs

In a previous study, it was shown that acylation and deacylation steps of wild-type GAPN could be kinetically resolved and that

Table 3 Kinetic parameters of the acylation step for the T244S, T244V and K178A GAPNs

Initial velocities of the reaction catalysed by mutated GAPNs were measured in 50 mM Tes buffer, pH 8.2, and 5 mM 2-mercaptoethanol at 25 °C. Previous enzyme activity measurements with either D,L-G3P or D-G3P showed that both enantiomeric forms equally behaved as efficient substrates for the wild-type GAPN [2]. Therefore D,L-G3P was used as a substrate for mutated GAPN-catalysed reactions. K_m values for NADP and D,L-G3P were determined by fitting the experimental data to the Michaelis–Menten equation.

GAPN	NADP K_m (μM)	D,L-G3P K_m (μM)	k_{cat} (s^{-1})	Rate-limiting step
Wild-type*	25 ± 2*	490 ± 50*	790 ± 20*	Deacylation
T244S	10 ± 3	120 ± 14	0.27 ± 0.03	Acylation
T244V	–	–	~ 0.002†	Acylation
K178A	70 ± 6	12 ± 5‡	0.020 ± 0.002	Acylation

* Corresponding to rate constant and K_m values for the cofactor and the substrate in the acylation step and determined with D-G3P [2]. Substrate inhibition was described to be observed for [D-G3P] > 200 μM (see [2]). The acylation rate constant was determined at 10 °C. Therefore, to compare the k_{cat} values of the mutated GAPNs and k_{ac} value of the wild-type GAPN, the reported k_{ac} value of the wild-type was extrapolated from the value measured at 10 °C, assuming a 2.5-fold increase of the rate constant k_{ac} per 10 °C (from [2]).

† The k_{cat} value was too low to permit determination of K_m values for NADP and D,L-G3P.

‡ Substrate inhibition was observed for [D,L-G3P] > 150 μM.

deacylation was rate-limiting under steady-state conditions [2]. It was also demonstrated that the rate-determining step within deacylation was associated with hydrolysis, whereas hydride transfer was rate-determining in acylation. Therefore, before interpreting the steady-state kinetic data, we first determined whether the rate-limiting step was still associated with the deacylation step for mutated GAPNs. For that, experiments were carried out at pH 8.2 and 25 °C under the following conditions, i.e. T244S GAPN (4 and 8 μM), NADP (0.03 mM), D,L-G3P (1.5 mM); K178A GAPN (4 and 8 μM), NADP (1 mM), D,L-G3P (0.15 mM); T244V GAPN (4 and 8 μM), NADP (1 mM), D,L-G3P (0.2 mM). No burst of NADPH formation was observed irrespective of the mutated GAPN and the measured rate constants were similar to the rate values determined under steady-state conditions (see next paragraph). These results showed that the rate-limiting step is associated with the acylation step for T244S, T244V and K178A GAPNs in contrast with the wild-type (Table 3). More precisely, as shown below, the rate-limiting step in T244S and K178A GAPNs is associated with hydride transfer. Therefore, to analyse a possible effect of the mutations introduced at positions 178 and 244 in terms of change in the apparent affinity constant for the G3P substrate and in rate constants, only the k_{ac} (acetylation constant) value and the K_m value for G3P of the wild-type in the acylation step have been considered.

T244S GAPN

As shown in Table 3, substituting serine for Thr^{244} resulted in a 2-fold decrease in K_m for NADP with a value of 10 μM. An inhibitory effect was observed for [NADP] > 60 μM. The K_m value for D,L-G3P decreased by a factor of 4 and the k_{cat} value decreased drastically, by a factor of 2900, relative to the k_{ac} value of the wild-type (Tables 3 and 4). At optimum pH 8.2, the k_{cat} value was decreased by a factor of 2.1 when D-[1-^{2}H]G3P was used as a substrate (Table 4). This strongly suggested that hydride transfer is rate-limiting. Therefore the hydride rate constant is decreased 2900-fold compared with the wild-type. The pH–rate profile was then studied over a pH range 5–8.75 at a saturating concentration of 1.5 mM D,L-G3P and at a concentration of 30 μM NADP, where

Table 4 Parameters for the pH-dependence of the k_{cat} values for the T244S, T244V and K178A GAPNs

pK_{app} and k_{cat} values were deduced from non-linear regression analysis of experimental data obtained at 25 °C against a single pK_a model. The substrate isotope effects were determined as described in the Experimental section.

GAPN	pK_{app1}	pK_{app2}	k_{cat} (s^{-1})	Substrate isotopic effect
Wild-type*	6.2 ± 0.1	7.5 ± 0.1	790 ± 20*	2.7
T244S	6.8 ± 0.1	–	0.27 ± 0.03†	2.1
T244V‡	–	–	~0.002†	–
K178A	6.7 ± 0.1	–	0.020 ± 0.002†	2.1

* The acylation rate constant for the wild-type was extrapolated from the value measured at 10 °C (from [2]).

† From Table 3.

‡ The k_{cat} value was too low to allow accurate determination of pK_a and substrate isotopic effect.

NADP does not behave as an inhibitor. As shown in Figure 3, the pH–k_{cat} profile exhibited a sigmoidal curve that can be related to the contribution of one ionizable group of pK_{app} 6.8 that must be deprotonated for acylation, and characterized by a k_{cat} of 0.27 s^{-1}. Compared with wild-type, pK_{app} of 6.8 would correspond to that of catalytic Cys[302]. The fact that the pH–k_{cat} profile depends on Cys[302] pK_{app} and not on Glu[268] pK_{app}, which was shown to be 7.6 in the wild-type [9], could be indicative of relative positioning of Cys[302] and Glu[268] in the T244S ternary Michaelis complex, slightly different from that found in the wild-type ternary complex.

T244V and K178A GAPNs

The kinetic parameters are summarized in Table 3. The T244V substitution led to a drastic 250 000-fold decrease of the k_{cat} value. The k_{cat} value of 2×10^{-3} s^{-1} was so low that determination of K_m values for NADP and D,L-G3P was not possible. The k_{cat} value for K178A GAPN was strongly reduced by a factor of 25 000 and the K_m values for NADP and D,L-G3P were 3-fold higher and 40-fold lower respectively, with respect to the wild-type. The large decrease in the D,L-G3P K_m value remains to be explained. Under steady-state conditions at optimum pH 8.2, a substrate kinetic isotopic effect of 2.1 was observed with D-[1-^{2}H]G3P (Table 4). Thus hydride transfer is also rate-limiting and is 25 000-fold less efficient than with the wild-type. The pH–rate profile was also studied over a pH range 5–9. k_{cat} values for K178A were determined at saturating concentrations of 0.15 mM D,L-G3P and 1 mM NADP respectively. As shown in Figure 3, the pH–k_{cat} profile exhibited a sigmoidal curve that can also be related to the contribution of one ionizable group of pK_{app} 6.7 and characterized by a k_{cat} value of 0.02 s^{-1}. Compared with the wild-type, pK_{app} of 6.7 would correspond to that of catalytic Cys[302], a value similar to that determined for T244S GAPN.

Structure of the T244S apo-like form

The $(2F_o - F_c)$ electron-density map is well defined for all of the structure. Difference maps revealed the presence of NADP in the four monomers. Three sulfate ions coming from the crystallization medium have also been identified in monomer D, whereas only two were present in monomer B, and one in each of monomers A and C. The sulfate anion whose position is conserved in all four monomers occupies the same location as the sulfate anion SO_4a found in the wild-type apo structure (Apo1 and Apo2 [15,12]), while the other is located on the protein surface.

The least-squares superimpositions involving the 474 Cα atoms of one subunit of the apo-like wild-type [15] with each subunit of the T244S GAPN structure result in r.m.s.d. values less than 0.29 Å, showing that the overall structures are very close. Local differences are limited to solvent-exposed regions, mobile loops and to the active-site region. In the wild-type structure, Thr[244] is located at the end of a β-strand and its β-hydroxy group is hydrogen-bonded to the ε-amino group of Lys[178], a residue located in an α-helix. In the T244S structure, the β-hydroxy group of

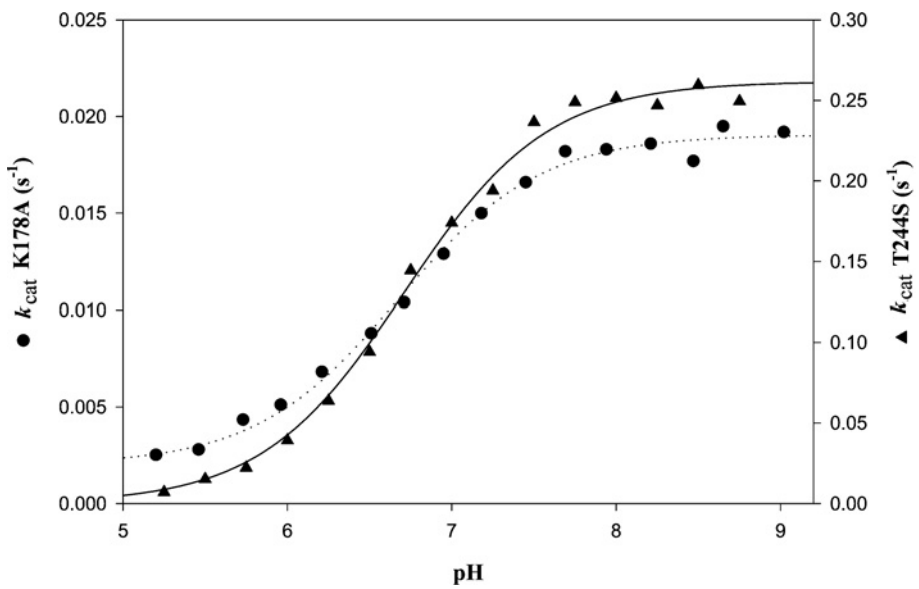

Figure 3 pH-dependence of the steady-state rate constant k_{cat} for K178A and T244S GAPNs

pH-dependence of k_{cat} was studied over the pH range 5.25–8.75 for T244S GAPN or 5.25–9.00 for K178A GAPN with a mixed reaction buffer consisting of 120 mM Tricine, 30 mM imidazole and 30 mM ethanoic acid at a constant ionic strength of 0.15 M. The other experimental conditions were as follows: 0.15 mM D,L-G3P, 1 mM NADP and 1.65 μM K178A GAPN; and 1.5 mM D,L-G3P, 0.03 mM NADP and 0.5 μM T244S GAPN. Data for T244S (▲) and K178A (●) GAPNs were best fitted by non-linear regression analysis against a single pK_{app} model, identified by the best-fit theoretical curves (solid line and dotted line respectively). S.E.M. on each experimental point was less than 5 %.

Ser^{244} adopts the same conformation and its interaction with Lys^{178} is conserved. The quality of the ($2F_o - F_c$) electron-density map is good enough to model the NMN moiety of the NADP molecule (Figure 1B). In particular, the pyridinium ring adopts a conformation, clearly different from that depicted for wild-type GAPN–NADP and $ALDH_2$–NAD binary complexes which was described to be suitable for an efficient hydride transfer [17]. In the T244S GAPN, the pyridinium ring is stabilized through van der Waals interactions with Cys^{302}, Pro^{167} and Leu^{174}. Cys^{302} is located after an α-helix, Pro^{167} lies at the end of a β-strand, and Leu^{174} is located on an α-helix. Moreover, the conformation of the side chain of catalytic Cys^{302} is closer to that found in the wild-type apo form than in the wild-type–NADP complex and the salt bridge between Arg^{459} and Glu^{268} remains present, albeit that NADP is bound (Figure 1A).

Finally, although the side chain of Arg^{301} was shown to bind the sulfate anion, called SO_4a, in the wild-type apo structures (Apo1 and Apo2 [12,15]) and was shown to both contribute to G3P binding and be involved in the efficient positioning of G3P relative to Cys^{302} within the ternary complex GAPN–NADP–G3P [26], it is positioned opposite to the SO_4a anion corresponding to the C-3 phosphate of G3P and interacts with the carbonyl groups of Gly^{294} and Ala^{293}. It is probable that the conformation adopted by the side chain of Arg^{301} in the binary complex corresponds instead to an alternative conformation which is not representative of the positioning of its guanidinium group within the competent wild-type ternary complex. Indeed, no significant K_m change for G3P accompanies the drastic decrease of the acylation rate observed for the T244S GAPN in contrast with what was observed for the R301L GAPN [26].

DISCUSSION

A key aspect of the chemical mechanism of the CoA-independent ALDH family is the requirement of a conformational isomerization of the NMN(H) portion of the cofactor after the oxidoreduction process to allow Glu^{268} to play its role in the deacylation step [18]. The fact that the acylation step in GAPN, and also many other CoA-independent ALDHs, is not rate-limiting and is efficient implies several prerequisites for this step. One of those relates to the optimal positioning of the nicotinamide ring towards the hemithioacetal within the ternary acylating complex. Several X-ray structures of binary ALDH–NAD(P) complexes reveal a great conformational flexibility of the NMN portion of the NAD(P) molecule, in particular of the nicotinamide ring (see, e.g., [11,14–15]). However, once the transient hemithioacetal intermediate is formed, the NMN moiety, in particular in GAPN, must be positioned such that an efficient and stereospecific transfer of hydride ion occurs towards C-4 of the nicotinamide ring. As indicated in the Introduction, invariant Thr^{244} is postulated to play a major role in the positioning of the nicotinamide ring within the ternary complex of CoA-independent ALDHs. The kinetic and structural data reported here on GAPN strongly favour such an assumption, in particular of the critical role of the β-methyl group of Thr^{244}.

Role of the β-methyl group of Thr^{244}

Substitution of serine for Thr^{244} led to a change in the nature of the rate-limiting step which becomes associated with the acylation step. Hydride transfer becomes rate-limiting and its efficiency is strongly decreased by a factor of 2900 compared with the wild-type. This drastic effect could be the consequence of changes occurring in the location and orientation of the nicotinamide ring relative to the hemithioacetal intermediate within the ternary complex, thereby preventing an efficient hydride transfer. The T244S GAPN structure in the presence of NADP clearly shows that the absence of the β-methyl group leads to a unique stabilized position of the nicotinamide ring clearly distinct from that hypothesized for the 'hydride transfer conformation' in CoA-independent ALDHs including GAPN [10,15–17]. The crystal structure presented herein is likely to be representative of the position occupied by the nicotinamide ring within the T244S GAPN–NADP complex in solution. This is in agreement with the fact that: (i) the formation of the binary complex T244S GAPN–NADP is not able to promote the chemical activation of Cys^{302} (its pK_{app} remains around 9) in contrast with what was observed for the wild-type [9], and (ii) the salt bridge between Arg^{459} and Glu^{268}, which is considered typical of the apo form [12], is still present in the X-ray binary complex structure.

Determination of the structure of a hemithioacetal intermediate is not possible because of its transient nature. If we assume that the nicotinamide conformation in the T244S hemithioacetal intermediate–NADP complex is the one observed in the crystal structure of the binary complex T244S GAPN–NADP, the poor efficiency of the hydride transfer could be explained by non-optimal positioning of the nicotinamide ring relative to the hemithioacetal intermediate. The 0.6-unit increase in pK_{app} of Cys^{302} compared with the wild-type, which is similar to the contribution of the positively charged nicotinamide ring in lowering the pK_{app} of Cys^{302} in the wild-type [9], can be also interpreted as the consequence of positioning of the nicotinamide ring relative to Cys^{302} slightly different from that in the wild-type acylating ternary complex. Therefore the role of the β-methyl group of Thr^{244} in the wild-type would be to mainly allow the nicotinamide ring to adopt a conformation suitable for an efficient hydride transfer.

An alternative explanation would relate to the positioning of the C-1 hydroxylate of the hemithioacetal intermediate relative to the oxyanion hole rendering it unsuitable for hydride transfer. However, this latter assumption is rather unlikely. First, the apparent affinity constant of T244S GAPN for G3P is not significantly changed. Secondly, whatever the X-ray structures considered, including those of the binary complex T244S GAPN–NADP, the apo-like wild-type and the ternary thioacylenzyme intermediate, the side chain of Asn^{169} involved in the oxyanion hole formation is always similarly positioned in all the structures [15,18].

Role of the β-hydroxy group of Thr^{244}

As mentioned in the Introduction, the Thr^{244} β-hydroxy group, which is hydrogen-bonded to the Lys^{178} ε-amino group, can help the β-methyl group of Thr^{244} to position the nicotinamide ring in a conformation suitable for hydride transfer. The T244V substitution was therefore intended to (i) determine the consequence of the loss of the hydrogen bond between the Thr^{244} β-hydroxy group and the Lys^{178} ε-amino group, and (ii) to introduce a valine residue invariant at this position in CoA-dependent ALDHs whose acylation step was shown to be as efficient as in GAPN [27]. Removing the β-hydroxy group in fact drastically alters the catalytic properties of the enzyme. The efficiency of the rate-limiting acylation step is decreased 250000-fold and 86-fold compared with the wild-type and T244S GAPNs respectively. Although it was not possible to determine whether hydride transfer remained rate-determining within the acylation step because of the very low k_{cat} value, the larger decrease of k_{cat} probably originates from the disruption of the hydrogen-bond interaction between the

residues at positions 244 and 178, thus leading to formation of an inefficient T244V ternary complex. However, one cannot exclude the possibility that the very low k_{cat} value of T244V GAPN is also due to additional structural changes induced by the presence of a valine residue in the hydrophilic environment of the GAPN active site.

The substitution of alanine for the counterpart residue Lys^{178} also appears to be informative and complementary to the studies carried out on T244S GAPN. In fact, the K178A and T244S GAPNs exhibited very similar catalytic properties. First, the rate-limiting step is associated with hydride transfer and a 25 000-fold decrease of the k_{cat} value was observed. Secondly, the pK_{app} values for Cys^{302} are equivalent in both ternary complexes, i.e. 6.7 compared with 6.8. Therefore it is tempting to interpret these results in a similar way to that developed in the preceding section for the T244S GAPN. So, the disruption of the Thr^{244}–Lys^{178} hydrogen-bond interaction by substituting either valine for Thr^{244} or alanine for Lys^{178} would alter the positioning of Thr^{244}, in particular of its β-methyl group and thus of the nicotinamide ring that could explain the very poor efficiency of the hydride transfer.

Relevance to the two-step catalytic mechanism

The major feature that has emerged from the present study lies in the critical contribution of the β-methyl group of invariant Thr^{244} in the efficiency of the GAPN acylation step. It probably contributes to formation of a transient hemithioacetal intermediate with an adequate positioning of the nicotinamide ring to allow an efficient hydride transfer. Such a role is expected to be general for all the members of the CoA-independent ALDH family. This is supported further by the presence of an invariant valine residue at position 244 in the CoA-dependent ALDH family. In these ALDHs, position 178 is mostly occupied by a methionine residue. Thus it is tempting to propose that one of the two methyl groups of the β-branched side chain of Val^{244} is positioned like that of β-methyl of Thr^{244} and therefore fulfils a similar function thanks to the other methyl group of Val^{244} which could interact via hydrophobic interactions with the side chain of residue 178. Such a hypothesis remains to be validated. In addition to Thr^{244}, the side chain of invariant Glu^{399} was shown to play an essential role by anchoring the NMN ribose through hydrogen bonds with the hydroxy groups of the ribose [28]. Lastly, it was also hypothesized that the negative charge of the tetrahedral oxyanion intermediate participates in the efficient positioning of the positively charged nicotinamide ring within the ternary complex hemithioacetal intermediate–NAD(P) [18]. Taken together, this probably delineates a pattern of interactions that stabilizes an efficient 'hydride transfer conformation' of the NMN moiety of the cofactor, once the transient hemithioacetal intermediate is formed.

Finally, recent structural data on the thioacyl intermediate of GAPN suggested that a low energetic barrier exists between the conformations adopted by the NMN(H) moiety during the two-step catalytic cycle of the CoA-independent ALDHs [18]. Based on the structure of the crystalline binary complex T244S GAPN–NADP, we propose that the β-methyl group of Thr^{244} might also play a role in the efficiency of the conformational isomerization of the NMNH after hydride transfer.

We are grateful to S. Boutserin for her very efficient technical help. We also thank Dr Van Dorsselear and Dr G. Chevreux for mass determination and Dr S. Sonkaria for careful reading of the manuscript. A. P. was fellow of the French Ministère de la Recherche et des Nouvelles Technologies (MRNT). This research was supported by the Centre National de la Recherche Scientifique, the French Ministère de la Recherche et de l'Enseignement Supérieur, the University Henri Poincaré Nancy I, the IFR 111 Bioingénierie and local funds from the Région Lorraine.

REFERENCES

1 Wang, X. and Weiner, H. (1995) Involvement of glutamate 268 in the active site of human liver mitochondrial (class 2) aldehyde dehydrogenase as probed by site-directed mutagenesis. Biochemistry **34**, 237–243
2 Marchal, S., Rahuel-Clermont, S. and Branlant, G. (2000) Role of glutamate-268 in the catalytic mechanism of nonphosphorylating glyceraldehyde-3-phosphate dehydrogenase from *Streptococcus mutans*. Biochemistry **39**, 3327–3335
3 Vallari, R. C. and Pietruszko, R. (1981) Kinetic mechanism of the human cytoplasmic aldehyde dehydrogenase E1. Arch. Biochem. Biophys. **212**, 9–19
4 Shone, C. C. and Fromm, H. J. (1981) Steady-state and pre-steady-state kinetics of coenzyme A linked aldehyde dehydrogenase from *Escherichia coli*. Biochemistry **20**, 7494–7501
5 Söhling, B. and Gottschalk, G. (1993) Purification and characterization of a coenzyme-A-dependent succinate-semialdehyde dehydrogenase from *Clostridium kluyveri*. Eur. J. Biochem. **212**, 121–127
6 Farres, J., Wang, T. T., Cunningham, S. J. and Weiner, H. (1995) Investigation of the active site cysteine residue of rat liver mitochondrial aldehyde dehydrogenase by site-directed mutagenesis. Biochemistry **34**, 2592–2598
7 Vedadi, M., Szittner, R., Smillie, L. and Meighen, E. (1995) Involvement of cysteine 289 in the catalytic activity of an NADP$^+$-specific fatty aldehyde dehydrogenase from *Vibrio harveyi*. Biochemistry **34**, 16725–16732
8 Vedadi, M. and Meighen, E. (1997) Critical glutamic acid residues affecting the mechanism and nucleotide specificity of *Vibrio harveyi* aldehyde dehydrogenase. Eur. J. Biochem. **246**, 698–704
9 Marchal, S. and Branlant, G. (1999) Evidence for the chemical activation of essential Cys-302 upon cofactor binding to nonphosphorylating glyceraldehyde 3-phosphate dehydrogenase from *Streptococcus mutans*. Biochemistry **38**, 12950–12958
10 Steinmetz, C. G., Xie, P., Weiner, H. and Hurley, D. T. (1997) Structure of mitochondrial aldehyde dehydrogenase: the genetic component of ethanol aversion. Structure **5**, 701–711
11 Johansson, K., El-Ahmad, M., Ramaswamy, S., Hjelmqvist, L., Jörnvall, H. and Eklund, H. (1998) Structure of betaine aldehyde dehydrogenase at 2.1 Å resolution. Protein Sci. **7**, 2106–2117
12 Cobessi, D., Tête Favier, F., Marchal, S., Branlant, G. and Aubry, A. (2000) Structural and biochemical investigations of the catalytic mechanism of an NADP-dependent aldehyde dehydrogenase from *Streptococcus mutans*. J. Mol. Biol. **300**, 141–152
13 Marchal, S., Cobessi, D., Rahuel-Clermont, S., Tete-Favier, F., Aubry, A. and Branlant, G. (2001) Chemical mechanism and substrate binding sites of NADP-dependent aldehyde dehydrogenase from *Streptococcus mutans*. Chem. Biol. Interact. **130–132**, 15–28
14 Liu, Z. J., Sun, Y. J., Rose, J., Chung, Y. J., Hsiao, C. D., Chang, W. R., Kuo, I., Perozich, J., Lindahl, R., Hempel, J. and Wang, B. C. (1997) The first structure of an aldehyde dehydrogenase reveals novel interactions between NAD and the Rossmann fold. Nat. Struct. Biol. **4**, 317–326
15 Cobessi, D., Tête Favier, F., Marchal, S., Azza, S., Branlant, G. and Aubry, A. (1999) Apo and holo crystal structures of an NADP-dependent aldehyde dehydrogenase from *Streptococcus mutans*. J. Mol. Biol. **290**, 161–173
16 Moore, S. A., Baker, H. M., Blythe, T. J., Kitson, K. E., Kitson, T. M. and Baker, E. N. (1998) Sheep liver cytosolic aldehyde dehydrogenase: the structure reveals the basis for the retinal specificity of class 1 aldehyde dehydrogenases. Structure **6**, 1541–1551
17 Perez-Miller, S. J. and Hurley, T. D. (2003) Coenzyme isomerization is integral to catalysis in aldehyde dehydrogenase. Biochemistry **42**, 7100–7109
18 D'Ambrosio, K., Pailot, A., Talfournier, F., Didierjean, C., Benedetti, E., Aubry, A., Branlant, G. and Corbier, C. (2006) The first crystal structure of a thioacylenzyme intermediate in the ALDH family: new coenzyme conformation and relevance to catalysis. Biochemistry **45**, 2978–2986
19 Corbier, C., Mougin, A., Mely, Y., Adolph, H. W., Zeppezauer, M., Gerard, D., Wonacott, A. and Branlant, G. (1990) The nicotinamide subsite of glyceraldehyde-3-phosphate dehydrogenase studied by site-directed mutagenesis. Biochimie **72**, 545–554
20 Otwinowski, Z. and Minor, W. (1997) Processing of X-ray diffraction data collected in oscillation mode. Methods Enzymol. **276**, 307–326
21 Brünger, A. T., Adams, P. D., Clore, G. M., DeLano, W. L., Gros, P., Grosse-Kunsteleve, R. W., Jiang, J. S., Kuszewski, J., Nilges, M., Pannu, N. S. et al. (1998) Crystallography & NMR system: a new software suite for macromolecular structure determination. Acta Crystallogr. Sect. D Biol. Crystallogr. **54**, 905–921
22 Reference deleted
23 Laskowsky, R. A., MacArthur, M. W., Moss, D. S. and Thornton, J. M. (1993) PROCHECK: a program to check the stereochemical quality of protein structures. J. Appl. Crystallogr. **26**, 283–291
24 Koradi, R., Billeter, M. and Wüthrich, K. (1996) MOLMOL: a program for display and analysis of macromolecular structures. J. Mol. Graphics **14**, 51–55

25 Esnouf, R. M. (1999) Further additions to MolScript version 1.4, including reading and contouring of electron-density maps. Acta Crystallogr. Sect. D Biol. Crystallogr. **55**, 938–940

26 Marchal, S. and Branlant, G. (2002) Characterization of the amino acids involved in substrate specificity of nonphosphorylating glyceraldehyde-3-phosphate dehydrogenase from *Streptococcus mutans*. J. Biol. Chem. **277**, 39235–39242

27 Stines-Chaumeil, C., Talfournier, F. and Branlant, G. (2006) Mechanistic characterization of the MSDH (methylmalonate semialdehyde dehydrogenase) from *Bacillus subtilis*. Biochem. J. **395**, 107–115

28 Ni, L., Sheikh, S. and Weiner, H. (1997) Involvement of glutamate 399 and lysine 192 in the mechanism of human liver mitochondrial aldehyde dehydrogenase. J. Biol. Chem. **272**, 18823–18826

Received 6 June 2006/21 August 2006; accepted 8 September 2006
Published as BJ Immediate Publication 8 September 2006, doi:10.1042/BJ20060843